An Intercomparison of Radiation Codes for Retrieving Upper-Tropospheric Humidity in the 6.3-μm Band: A Report from the First GVaP Workshop

B. Soden,[a] S. Tjemkes,[b] J. Schmetz,[b] R. Saunders,[c] J. Bates,[d] B. Ellingson,[e] R. Engelen,[f] L. Garand,[g] D. Jackson,[d] G. Jedlovec,[h] T. Kleespies,[i] D. Randel,[j] P. Rayer,[k] E. Salathe,[l] D. Schwarzkopf,[a] N. Scott,[m] B. Sohn,[n] S. de Souza-Machado,[o] L. Strow,[o] D. Tobin,[p] D. Turner,[g] P. van Delst,[p] T. Wehr[o]

ABSTRACT

An intercomparison of radiation codes used in retrieving upper-tropospheric humidity (UTH) from observations in the $v2$ (6.3 μm) water vapor absorption band was performed. This intercomparison is one part of a coordinated effort within the Global Energy and Water Cycle Experiment Water Vapor Project to assess our ability to monitor the distribution and variations of upper-tropospheric moisture from spaceborne sensors. A total of 23 different codes, ranging from detailed line-by-line (LBL) models, to coarser-resolution narrowband (NB) models, to highly parameterized single-band (SB) models participated in the study. Forward calculations were performed using a carefully selected set of temperature and moisture profiles chosen to be representative of a wide range of atmospheric conditions. The LBL model calculations exhibited the greatest consistency with each other, typically agreeing to within 0.5 K in terms of the equivalent blackbody brightness temperature (T_b). The majority of NB and SB models agreed to within ±1 K of the LBL models, although a few older models exhibited systematic T_b biases in excess of 2 K. A discussion of the discrepancies between various models, their association with differences in model physics (e.g., continuum absorption), and their implications for UTH retrieval and radiance assimilation is presented.

[a]NOAA/GFDL, Princeton, New Jersey.
[b]EUMETSAT, Darmstadt, Germany.
[c]ECMWF, Reading, United Kingdom.
[d]NOAA/CDC, Boulder, Colorado.
[e]University of Maryland at College Park, College Park, Maryland.
[f]Colorado State University, Fort Collins, Colorado.
[g]AES, Dorval, Quebec, Canada.
[h]NASA/MSFC, Huntsville, Alabama.
[i]NOAA/NESDIS, Washington, D.C.
[j]CIRA/CSU, Fort Collins, Colorado.
[k]Meteorological Office, Bracknell, United Kingdom.
[l]University of Washington, Seattle, Washington.
[m]CNRS/LMD, Palaiseau, France.
[n]Seoul National University, Seoul, South Korea.
[o]University of Maryland–Baltimore County, Baltimore, Maryland.
[p]University of Wisconsin—Madison, Madison, Wisconsin.
Corresponding author address: Dr. Brian J. Soden, Princeton University, Forrestal Campus, U.S. Route 1, P.O. Box 308, Princeton, NJ 08542-0308.
E-mail: bjs@gfdl.gov
In final form 12 August 1999.

1. Introduction

Water vapor is widely recognized to be a key climate variable, serving to link an assortment of complex and poorly understood processes. Reducing current uncertainties involving water vapor in the climate system requires accurate global measurement, modeling, and long-term prediction of water vapor. Toward this end, the Global Energy and Water Cycle Experiment (GEWEX) Global Water Vapor Project (GVaP) was given the responsibility to "establish an accurate and validated water vapor climatology on the relevant space and time scales" (Chahine 1997). To help meet this research objective, a series of workshops are planned that will target key areas of uncertainty. The first of these meetings, a GVaP Workshop on Upper Tropospheric Humidity Measurements and Retrievals, was held in Darmstadt, Germany, on 2–3 June 1998 at the European Organization for the Exploitation of Meteorological Satellites.

The purpose of the workshop was to intercompare top-of-atmosphere radiances in the 6.3-μm water vapor absorption band as simulated by different radiative transfer codes. At present there are several spaceborne sensors that measure the upwelling radiance in this spectral range to retrieve information on the moisture content of the upper troposphere. The derivation of upper-tropospheric humidity (UTH) from these observations is being done at a variety of institutes throughout the world (Schmetz and Turpeinen 1989; Soden and Bretherton 1993; Stephens et al. 1996; Salathe and Hartmann 1997; Spencer and Braswell 1997; Garand and Hallé 1997; Berg et al. 1998; Jedlovec et al. 2000; Chaboureau et al. 1998). Common to all UTH retrieval methods is a dependence on "forward" radiative transfer calculations. Likewise, direct assimilation of water vapor radiances into numerical prediction models (e.g., Eyre et al. 1993; Garand et al. 1997; Derber and Wu 1998) also requires accurate and efficient forward models.

There are a number of models, of varying origins and levels of complexity, that can be used to perform such calculations. Unfortunately, little is known regarding the consistency among various radiative transfer codes despite the fact that differences between existing radiation codes can have a substantial effect on the retrieval and assimilation of UTH information. While differences between various satellite-derived UTH climatologies are known to exist (e.g., Stephens et al. 1996; Spencer and Braswell 1997; Engelen and Stephens 1998), the extent to which these are attributable to discrepancies in the transmittance models used for the retrieval is unknown. Given the importance of accurate radiation codes for both climatological assessment of UTH as well as operational utilization of water vapor radiance measurements, a comprehensive comparison of existing models is clearly needed. The first GVaP workshop addressed this need by providing a systematic intercomparison of radiative transfer codes using identical spectral response functions and a carefully selected set of 43 representative temperature and humidity profiles. The objective of this comparison is to evaluate the consistency between various models rather than their absolute accuracy. The next section documents the different models that participated in the comparison as well as the atmospheric profile dataset used in the study. The major findings of the workshop are presented in section 3, followed by a summary and recommendations for future GVaP workshops in section 4.

2. Description of radiation codes and atmospheric profiles

Table 1 summarizes the models that participated in the comparison. Listed with each model is information about its line parameters, type of continuum parameterizations for molecular oxygen and water vapor, references, and the investigators who submitted the results. A total of 23 different models, ranging from detailed line-by-line (LBL) models to coarse-resolution narrowband (NB) models to highly parameterized single-band (SB) models, participated in the intercomparison. Each model used the same spectral response function representing channel 12 on the High Resolution Infrared Sounder (HIRS) from the *NOAA-12* spacecraft. The spectral response function for this channel peaks at approximately 6.7 μm near the center of the P branch of the $\nu 2$ absorption band

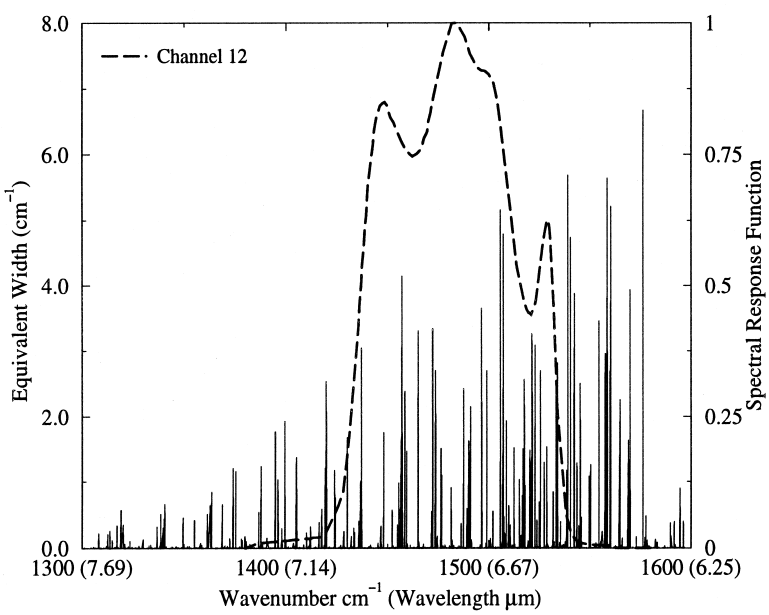

FIG. 1. The normalized spectral response function (dashed line) for channel 12 (6.7 μm) on the *NOAA-12* spacecraft superimposed upon the equivalent widths of water vapor absorption lines in the $\nu 2$ band. The equivalent widths (solid lines) were calculated using spectroscopic information from the HITRAN-92 database and correspond to an integrated water vapor mass concentration of 0.25 mol cm^{-2}, a pressure of 300 hPa, and a temperature of 240 K.

TABLE 1. A list of radiative transfer models used in the comparison. The models are grouped according to their spectral resolution: LBL (1–10), NB (11–13), and SB (14–23). The contributor refers to the number key on the author affiliation list. Continuum O_2 indicates the oxygen continuum parameterization: x used to show results based on Thibault et al. (1997); y used to show results based on Timofeyev and Tonkov (1978). Continuum H_2O indicates the water vapor continuum parameterization. CKD refers to a version of the Clough–Kneizys–Davies continuum parameterization, Clough et al. (1989): ampersand (&), assumes Lorentz line shape for far wings, and number sign (#), same as that used in LOWTRAN-6; Kneizys et al. (1983). Line database refers to the line parameters used for LBL models: H = HITRAN (Rothman 1993); G = GEISA (Jacquinet-Husson et al. 1999), with the last two digits indicating the year database was released.

	Model	Contributor	Reference	Continuum		Line database
				O_2	H_2O	
1	GENLN2 4.0	k	Edwards (1992)	y	CKD 2.1	H96
2	4A LBL	m	Tournier et al. (1995)	y	CKD 2.1	G93
3	AES LBL	g	Turner (1995)	x	CKD 2.1	H96
4	GENLN2-UW	p	Edwards (1992)	y	CKD 2.1	H96
5	GFDL LBL	a	Schwarzkopf and Ramaswamy (1999)	y	CKD 2.1	H92
6	kCARTA CKD0	o	Strow et al. (1998)	y	CKD 0	H96
7	kCARTA CKD2.3	o	Strow et al. (1998)	y	CKD 2.3	H96
8	LBLRTM G97	b	Clough and Iacono (1995)	y	CKD 2.2	G97
9	LBLRTM L101	p	Clough and Iacono (1995)	y	CKD 2.2	H96
10	LBLRTM L42	p	Clough and Iacono (1995)	y	CKD 2.2	H96
11	MODTRAN3 1.5	d,n	Berk et al. (1989)	y	CKD 0	
12	UMD	e	Warner (1997)	None	CKD 2.1	
13	Streamer	l	Key (1997)	None	no	
14	Malkmus	f	Engelen and Stephens (1999)	None	CKD 2.2	MODTRAN
15	AES Fast	g	Garand et al. (1999)	x	CKD 2.1	AES LBL
16	HFFP	o	Joiner et al. (1998)	y	CKD 2.1	GENLN2
17	OPTRAN	i	McMillin et al. (1995)	y	CKD 2.2	LBLRTM
18	RTTOV-5	c	Saunders et al. (1999)	y	CKD 2.1	GENLN2
19	SRM	a	Soden and Bretherton (1993)	None	&	H92
20	SYNSATRAD	b	Tjemkes and Schmetz (1997)	*	CKD 2.2	LBLRTM
21	RTTOV-3	c	Eyre (1991)	None	#	HARTCODE
22	OTTM	a	Weinreb et al. (1981)	None	None	Neuendorfer (1977)
23	SIMRAD	h	Weinreb et al. (1981)	None	None	

(Fig. 1). In this portion of the infrared spectrum, water vapor is by far the dominant absorber. However, there are non-negligible contributions from O_2 and CH_4. Salathe and Smith (1996) estimate that the net contribution of the non-H_2O gases on the 6.7-μm radiance to be less than 0.5 K, with O_2 being the dominant non-H_2O absorber. The NB and LBL model transmittance calculations were explicitly convolved with the spectral response function in Fig. 1, whereas the SB models are constructed to contain this convolution implicitly within their transmittance functions (i.e., their transmittance functions are channel and satellite specific).

It is clear from Table 1 that different models often share common features, such as the line parameter database or continuum parameterization. For example,

most SB models use coefficients derived from higher-resolution (NB or LBL) calculations (the model used to derive the SB transmittance coefficients is listed under "Line database" in Table 1). Similarly, a majority of the LBL models use the HITRAN-96 line database and some version of the Clough–Kneizys–Davies (CKD) water vapor continuum parameterization (Clough et al. 1989). However, there are exceptions. For example, LBLRTM calculations have been performed with both the HITRAN-96 (models 9 and 10) and GEISA-97 (model 8) line parameters. Likewise, different models may use different versions of water vapor and oxygen continuum parameterizations or have varying vertical resolution. This diversity allows us to investigate the impact of different representations of current theory on the simulated radiance (e.g., the same model with different line parameters or continuum formulations), as well as different implementations of current theory (e.g., different models using identical line parameters).

The atmospheric profiles used in this comparison are a subset of the Television Infrared Observation Satellite (TIROS) Operational Vertical Sounder (TOVS) Initial Guess Retrieval (TIGR-2) profile dataset (Chedin et al. 1985; Escobar-Munoz 1993), which is a collection of radiosonde profiles carefully selected to portray a wide range of atmospheric conditions. A subset of 42 representative water vapor and temperature profiles were sampled from the 1761 profiles contained in the TIGR dataset and interpolated onto 101 uniformly spaced pressure levels. These levels are identical for all profiles and extend from 1100 to 0.005 hPa, with a typical spacing of 10–20 hPa. The overall mean of these 42 profiles provided the 43d profile used in the comparison. Above 300 hPa, the radiosonde humidity profiles were interpolated to a dataset of stratospheric water vapor profiles (starting at 100 hPa) derived from the Halogen Occultation Experiment. Further details regarding the development of this profile set can be found in Matricardi and Saunders (1999, manuscript submitted to *Appl. Opt.*). Finally, since many of the parameterized SB models have a specified vertical gridding that differs from model to model, it was not possible to perform this comparison on a uniform vertical coordinate. Therefore, the number of levels used in the calculations varied from model to model. However, every effort was made to ensure that the vertical interpolation of the atmospheric profiles to a particular model coordinate system was performed consistently (i.e., linear in log pressure). Additionally, calculations from one of the models that does have a flexible coordinate (LBLRTM) were performed with two vertical resolutions (which encompass most of the range of vertical resolutions among the models) to provide a rough estimate of the sensitivity to vertical resolution.

3. Results

a. Top of atmosphere radiance intercomparison

The equivalent blackbody brightness temperatures (hereafter referred to as brightness temperatures) calculated for all 43 profiles are presented for each of the 23 models in Fig. 2. To facilitate the comparison, the results are presented in terms of difference in T_b, relative to that computed by a reference model, as a function of the reference model T_b. Model 1 (GENLN2) was chosen as the reference model for the sole reason that it represents the median of the LBL calculations. It is important to note, however, that selection of GENLN2 as the reference in no way implies that it provides better agreement with observations. Indeed, establishing which of the LBL models is more accurate is a challenging task since many of the differences noted here are smaller than those that result from uncertainties in measuring the atmospheric state. The models are grouped into three categories in Fig. 2 according to their spectral resolution: LBL models (top), NB models (middle), and SB models (bottom). The T_b differences for all three groups of models were computed from the same model (GENLN2) to provide a common reference between each group. We note that, to a good approximation, the absolute T_b can be interpreted as the temperature field of the atmosphere on a water vapor isosteric surface (Soden and Bretherton 1993). More specifically, the T_b can be interpreted as the temperature of the profile at which the vertically integrated overburden of watervapor (along the line of sight) is ~0.2 mm. Thus, plotting the difference as a function of the reference T_b also provides information on the differing thermodynamic characteristics of the 43 profiles.

The bias in T_b averaged over the 43 profiles is listed in parentheses next to each model. Of the three categories of models, the LBL models (1–10) clearly exhibit the greatest degree of consistency with each other (note the differing scales between model groups). All LBL models, with the exception of model 2 (4A LBL; rms = 0.7 K), have rms differences with respect to GENLN2 of less than 0.5 K (Fig. 3). The av-

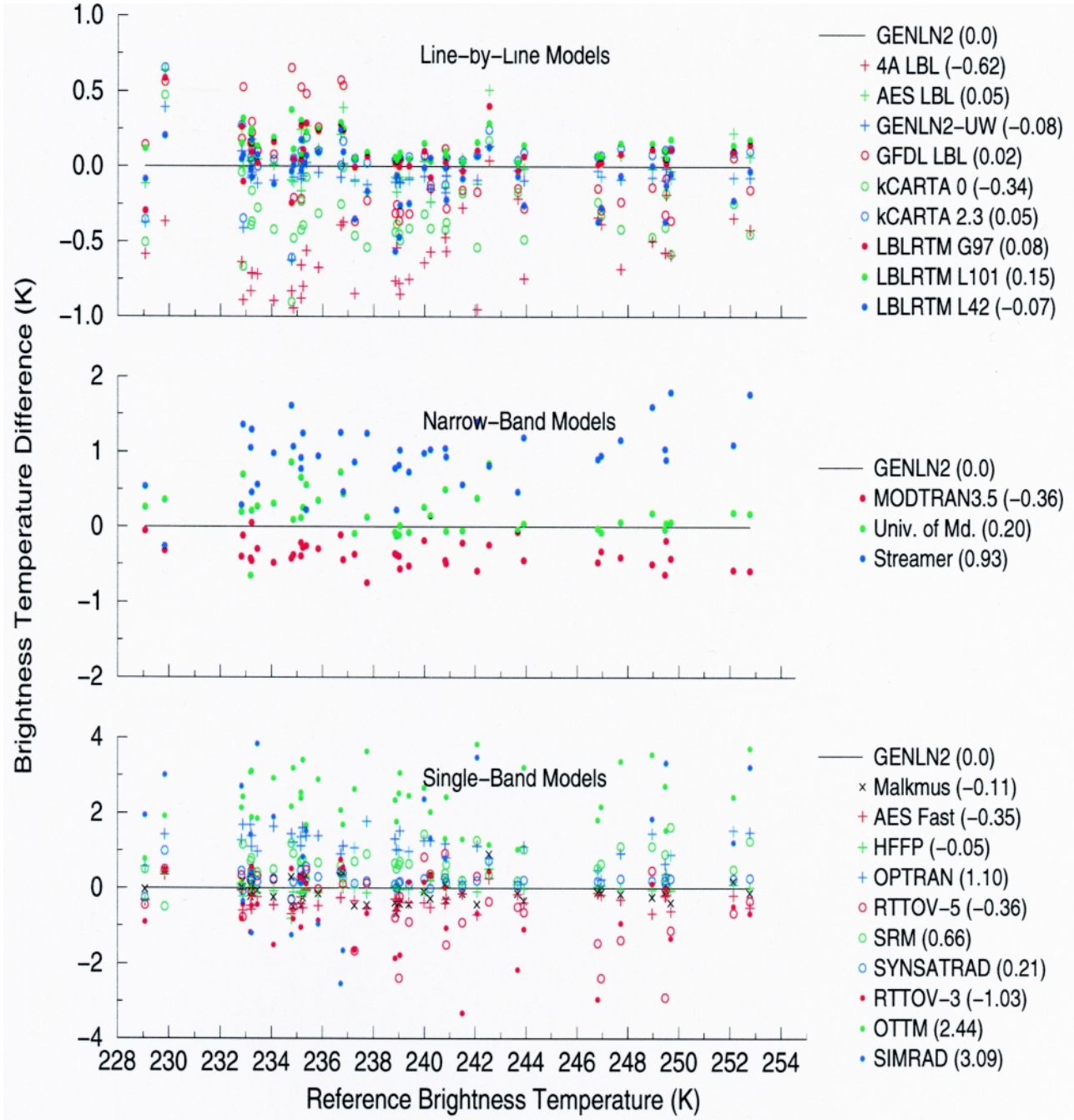

FIG. 2. Results of the radiative transfer model intercomparison grouped according to the spectral resolution of the model. The difference in T_b, computed with respect to the reference model (GENLN2), is plotted as a function of the reference model T_b for line-by-line models (top), narrowband models (middle), and single-band models (bottom) for all 43 atmospheric profiles. The bias in T_b relative to the reference model is listed in parentheses.

erage rms difference of the 10 LBL models is 0.25 K. A tendency for reduced scatter for warmer T_b is also apparent, suggesting greater consistency among LBL models for profiles with relatively dry upper tropospheres. While it is tempting to attribute the larger rms difference for model 2 to its different source of line parameters (GEISA vs HITRAN; cf. Table 1), the calculations from the LBLRTM using both the GEISA-97 database (model 8) and HITRAN-96 database (models 9 and 10) both exhibit much smaller rms differences with respect to GENLN2. This indicates that differences between the GEISA and HITRAN line

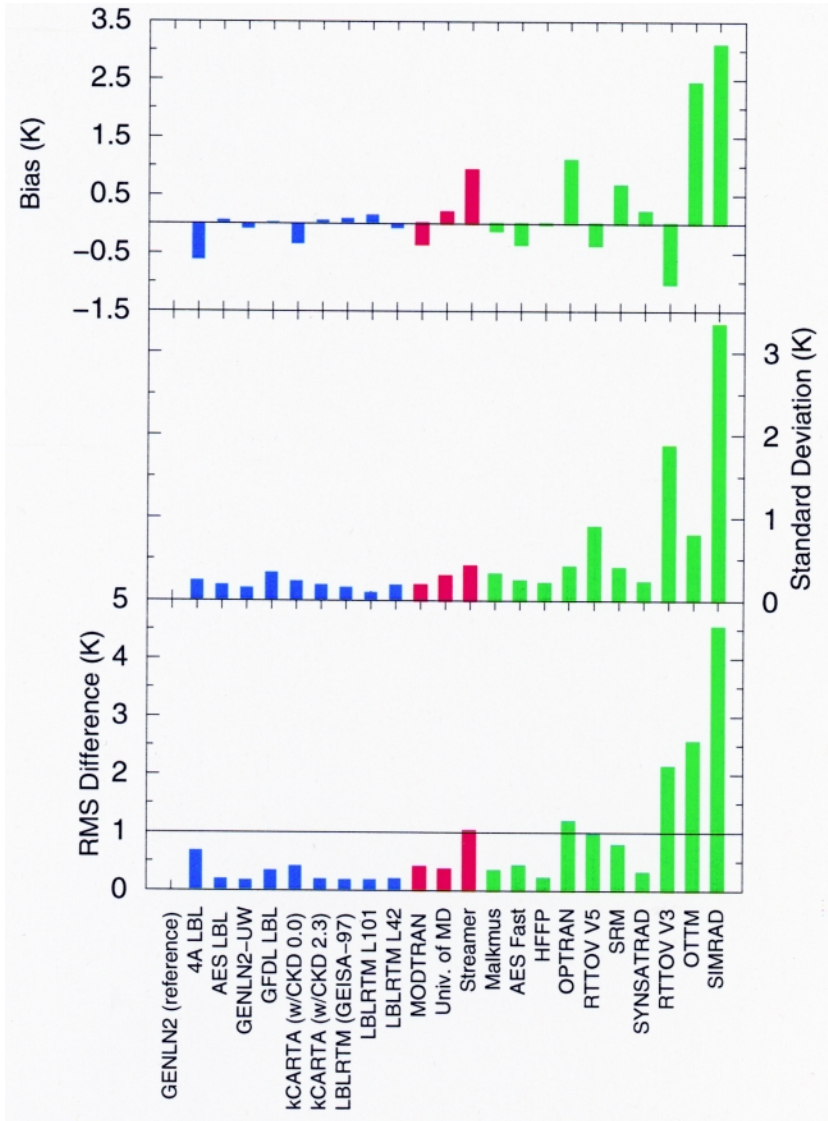

FIG. 3. The bias (top), std dev (middle), and rms difference (bottom) of the simulated brightness temperature (in K) for each model with respect to the reference LBL model (1–GENLN2).

parameters are not a significant source of discrepancy for radiance calculations in this spectral interval. However, when the H_2O continuum parameterization in model 2 (CKD 2.1) was adjusted to agree with High Resolution Interferometer Sounder measurements (taken under low humidity conditions), the rms difference with respect to GENLN2 was reduced from 0.7 to 0.3 K, indicating that even subtle differences in the parameterization of H_2O continuum absorption can be an important source of discrepancy in LBL calculations for this channel.

Relative to the LBL results, the NB models (11–13) exhibit somewhat larger intermodel variability. They also tend to have larger discrepancies with respect to GENLN2 calculations with rms differences ranging from ~0.4 to 1.0 K (Fig. 3a).

Of the three categories, the most variable results are found among the SB models. Since these models are the most computationally efficient, they are also the most widely used for radiance assimilation and UTH retrieval. The magnitude of scatter between the various SB models stands in direct contrast to the relative consistency among the LBL models. This indicates that while our theoretical treatment of the transmittance characteristics of this spectral region have converged, the implementation of that theory has not. Indeed, the SB calculations show a broad range of differences with respect to the reference LBL results (Fig. 3, bottom). Some SB models (e.g., 16 and 20) agree remarkably well with GENLN2, exhibiting rms differences comparable to those found in other LBL models, whereas other SB models (e.g., 21, 22, 23) have rms differences in excess of 2 K. It is encouraging, however, that much of the intermodel variability in this group is associated with a few outlying models that, in fact, tend to be either older models or outdated versions. For example, the models that exhibit the largest rms differences (22 and 23) are both derived from a nearly operational transmittance model developed at the National Environmental Satellite, Information and Data Service (NESDIS) (Weinreb et al. 1981), which lacks any explicit representation of water vapor continuum in the 6.3-μm band. In contrast, the current NESDIS operational model (17, OPTRAN) exhibits much better agreement with the reference LBL calculations. Similarly, the most recent version of RTTOV (version 5) exhibits noticeably smaller differences with respect to GENLN2 than does its predecessor (version 3). For a few profiles (e.g., profile 36) RTTOV-3 calculations differ significantly from those of RTTOV-5 (and most other models). Some of this difference stems from the fact that RTTOV-3 replaces the specific humidity profile above 300 hPa with an extrapolated profile that

is internally generated by the model. It is partly the elimination of this artificial feature, rather than a change in transmittance formulation, that is responsible for the improved performance of RTTOV-5.

Figure 3 (top) shows the difference in mean brightness temperature, averaged over the 43 atmospheric profiles, for each model relative to that computed from the reference LBL model (1). For the vast majority (21 out of 23) of models, the simulated brightness temperatures agree with the reference LBL calculations to within approximately 1 K. Exceptions are again evident for the older band models (22 OTTM and 23 SIMRAD), which exhibit biases in excess of 2 K. These larger biases reflect the absence of water vapor continuum absorption in the 6.3-μm region, resulting in systematically larger radiances relative to the other models.Again, the highest degree of commonality is found among the LBL models for which the majority agree to within 0.2 K. For reasons not completely understood, one LBL model (2) differs systematically from the others by roughly 0.7 K. The other outlying LBL model (kCARTA with CKD 0) uses an older version of the CKD water vapor continuum parameterization. Of the remaining eight LBL models, the largest discrepancy occurs for the same model (LBLRTM) integrated with two different vertical resolutions, 101 levels (model 9), and 42 levels (model 10). Thus, simply changing the vertical resolution of a model can alter the mean radiance by ~0.2 K. This sensitivity is not specific to the LBLRTM, but rather the issue of accurate vertical integration for a vertically inhomogenous atmosphere is a general one that applies to all models. This is an important consideration when comparing radiance calculations between general circulation models with differing vertical resolution, particularly when the number of levels is small.

Compared to the LBL models, the NB and SB models exhibit noticeably larger biases. However with the exception of the two older SB models (22 and 23), the remaining models exhibit biases with respect to the reference LBL results of less than 1 K. Unfortunately, this does not mean that the SB models agree with each other to within 1 K. For example, two of the more widely used operational models (RTTOV and OPTRAN) exhibit differences with respect to the reference LBL model of less than 1 K; however, the biases are of the opposite sign. Hence the relative difference between these two models is nearly 1.5 K for RTTOV-5 (2.0 K for RTTOV-3). As demonstrated below, such discrepancies lead to systematic biases when retrieving UTH as well as in direct assimilation of the water vapor radiances. In some situations, radiance correction schemes can be employed to remove known biases. For example, the improved initialization inversion retrieval scheme (Chedin et al. 1985), employs a "deltac correction," which relies on collocated satellite and radiosonde measurements to account for biases in the forward model. Such corrections, however, ultimately rely on the accuracy of the in situ humidity measurements, which generally are poor in the upper troposphere.

In general the agreement demonstrated here, particularly among the LBL models, is encouraging. It is emphasized, however, that consistency among the various radiative transfer models does not necessarily imply accuracy. Validation of radiative transfer models, especially of reference calculations produced by line-by-line models, can only be achieved through a comparison of radiative transfer calculations (based upon accurate observations of the input parameters, e.g., temperature and trace gas concentrations) with observed spectral radiances. The ability to perform such comparisons hinges on the existence of accurate in situ measurements as well as an accurate understanding of satellite instrument calibration and spectral characterization.

b. Effects of continuum absorption

Previous studies (e.g., Clough et al. 1992; Stephens et al. 1996) have noted that continuum absorption (i.e., absorption due to the wings of remote lines) from water vapor can play an important role in determining the atmospheric transmittance, even within the 6.3-μm band, which is actually dominated by line absorption (i.e., absorption in local lines). In addition to water vapor, continuum absorption by molecular oxygen also has a non-negligible influence on the atmospheric transmittance in this portion of the infrared spectrum. To assess the relative importance of H_2O and O_2 continuum absorption in existing radiative transfer models, calculations from both an LBL model (9) and an SB model (20) were repeated for no-H_2O continuum absorption and no-O_2 absorption. Results for the LBL model are plotted in Fig. 4. On average, inclusion of continuum absorption reduces the radiance at the top of the atmosphere by 1.71 K for water vapor and 0.3 K due to the oxygen continuum. The results from the SB model (20) give very similar results; water vapor continuum reduces the radiance by 1.68 K while oxygen continuum reduces it by 0.28 K. Thus the net contribution by both species is roughly 2 K, indicating that accurate treatment of continuum ab-

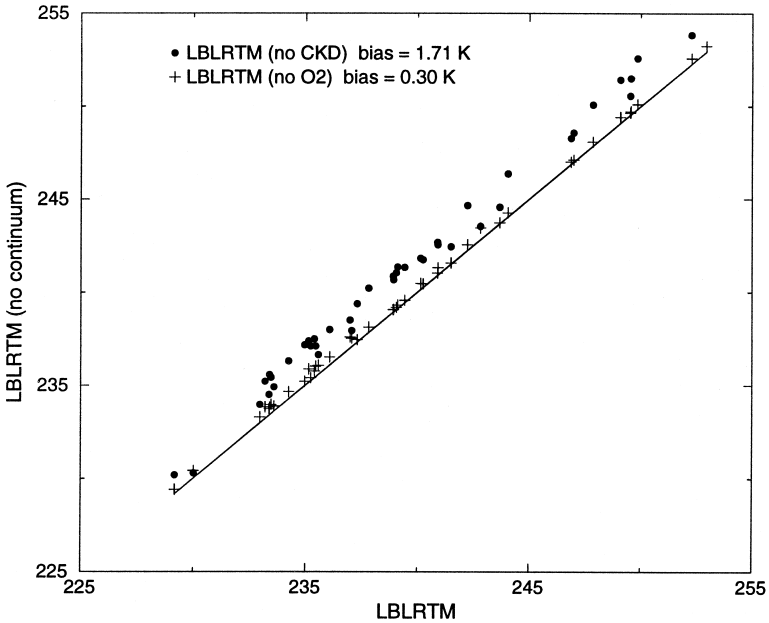

FIG. 4. A comparison of the brightness temperature (in K) simulated from the LBLRTM (model 9) vs those simulated using the same model without water vapor continuum absorption (no CKD) and without molecular oxygen continuum absorption (no O_2). The solid line represents perfect agreement.

sorption, particularly due to water vapor, is a necessity for reliable retrieval and assimilation of UTH information from satellite-observed 6.3-μm radiances. It is important to note, however, that the exact magnitude of continuum absorption remains somewhat uncertain and these numbers are subject to revision in the future as the parameterizations and our understanding evolve. For example, the calculations from the kCARTA LBL model were performed with two different versions of the CKD parameterization—versions 0 and 2.3. The mean radiance between runs of the same model with two different versions of the water vapor continuum differ by ~0.4 K, which is nearly 25% of the currently estimated (CKD 2.3) water vapor continuum contribution. The greater absorption provided by the CKD 0 relative to the more recent CKD schemes may also explain the negative radiance bias in MODTRAN3 v1.5 (Fig. 3), which also uses CKD 0.

To fully interpret these results, it is important to recognize that continuum absorption, as defined by CKD, refers to the "absorption, of slow spectral variation (compared with that for lines) which, when added to the local line contribution, provides agreement with observation." This is relevant to the current discussion since it implies that the continuum absorption and line absorption are inseparable. That is, the continuum absorption depends upon the line parameters and observational data used to derive it, as well as the definition of "local line contribution." This subtle point is often overlooked in model development, resulting in a mixing of line parameters and CKD versions (cf. Table 1).

c. Jacobian intercomparison

For variational (1D-Var) UTH retrievals or direct assimilation of radiances in an NWP model it is necessary to compute not only the "first guess" radiance from the model profiles (normally a 6-h forecast) but also the gradient of the transmittance model with respect to the input profile variables. This is commonly referred to as the Jacobian $H(\boldsymbol{X})$ and is a set of partial derivatives of the brightness temperature, T_b, with respect to all the profile variables,

$$H(\boldsymbol{X}) = \frac{\partial T_b(X)}{\partial(X)},$$

where $\boldsymbol{X}$ is the profile vector that for HIRS contains the temperature, water vapor, and ozone profiles either on fixed pressure levels for most fast models or on arbitrary pressure levels (e.g., model 17). Note surface temperature, humidity, and pressure are also part of the profile vector.

Five models (2, 15, 17, 18, 20) participated in a comparison of the gradient of their high resolution infrared Sounder-12 (HIRS-12) brightness temperatures with respect to water vapor for two extreme profiles, one tropical and one arctic. Only the water vapor profile was modified by reducing the specific humidity value by 10% at a single level and then computing the corresponding change in top-of-atmosphere T_b. This process was repeated individually for each level in the profile to construct the Jacobian $H(\boldsymbol{X})$.

The results are shown in Fig. 5a for a tropical profile and Fig. 5b for an arctic profile. The sensitivities plotted are the $\delta T_b(\boldsymbol{X})$ values for a $\delta\boldsymbol{X}$ of − 10% in specific humidity and the values have then been normalized by the pressure thickness of the layer to allow direct comparisons between the models with different vertical resolutions. As expected for the tropical profile the Jacobian has its largest value around 200 hPa showing where HIRS-12 is most sensitive to changes

in water vapor. For the arctic profile the sensitivity is much less (by an order of magnitude) and is over a much deeper layer. The overall shapes of the curves are similar for all the models. However, RTTOV-5 with only 43 levels does have a somewhat different behavior than the other three models, which all have more than 100 levels.

d. Impact on UTH retrieval

Any retrieval strategy depends heavily on the ability to accurately relate radiances to absorber concentrations. Therefore systematic differences in transmittance models will inevitably introduce differences in the derived products even when using the same retrieval method. Exceptions may occur when bias correction schemes, based upon collocated comparisons with in situ measurements, are used (e.g., Chedin et al. 1985). However such measurements depend critically upon the accuracy of the in situ measurements. Since water vapor typically reduces the upwelling radiance in this spectral region, a radiative transfer model that overpredicts the radiance would require erroneously larger amounts of water vapor to yield the correct brightness temperature. To illustrate the impact of errors in radiance calculations, consider the retrieval of Soden and Bretherton (1993), which relates the 6.7-μm T_b to the logarithm of UTH according to

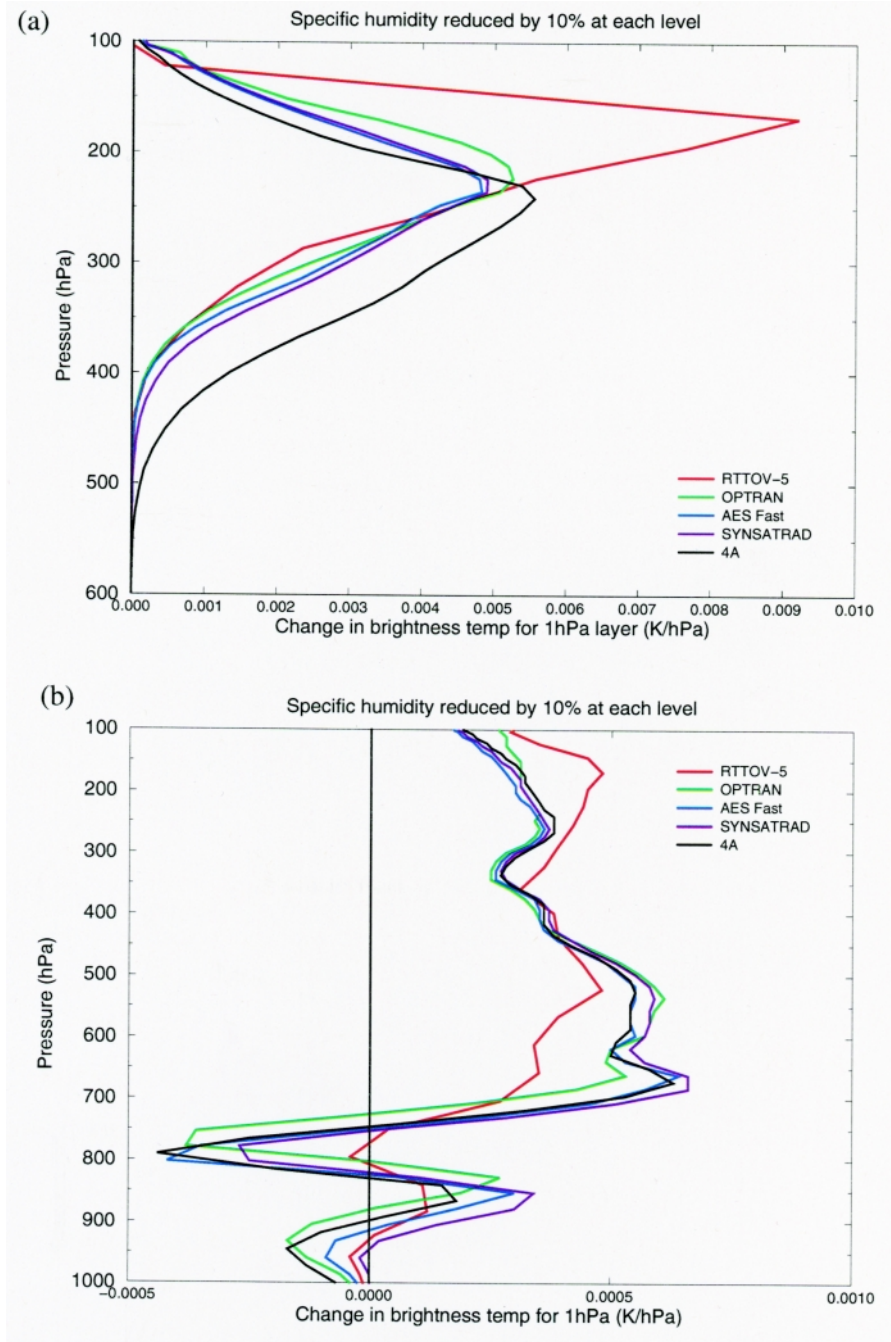

FIG. 5. Profiles of the change in brightness temperature resulting from a 10% reduction in specific humidity at each level for a tropical profile (top) and an arctic profile (bottom). Results are shown for five models (4A, RTTOV-5, OPTRAN, AES Fast, and SYNSATRAD).

$$\ln\left(\frac{\mathrm{UTH}\cdot p_o}{\cos\theta}\right) = a + bT_b, \qquad (1)$$

where θ is the satellite zenith angle and p_0 is a reference pressure. The coefficients a and b are determined by fitting this relation to radiative transfer calculations. Taking the discrete derivative of (1) yields

$$\left(\frac{\Delta\mathrm{UTH}}{\mathrm{UTH}}\right) = b\Delta T_b. \qquad (2)$$

For a typical value of $b = -0.12$ K^{-1}, Eq. (2) shows that a 1-K uncertainty in the simulated brightness tempera-

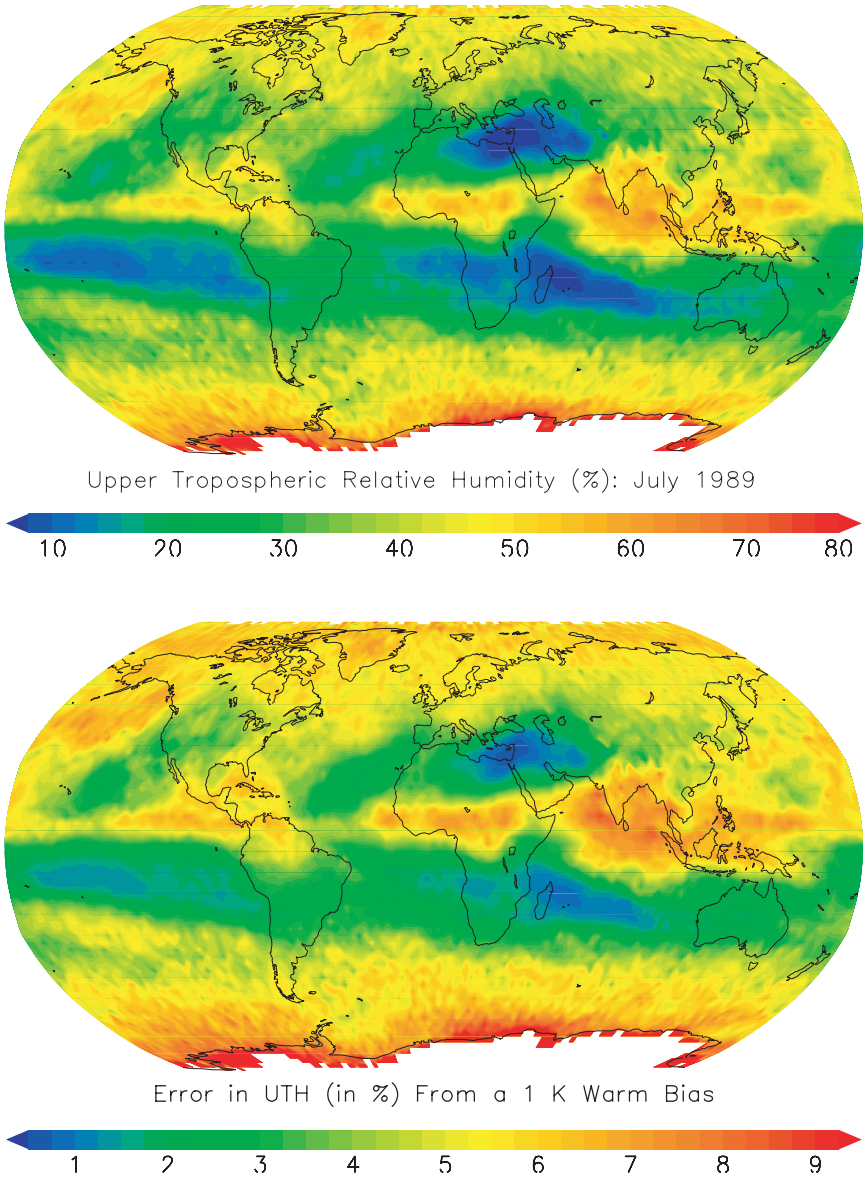

FIG. 6. (top) The distribution of upper-tropospheric relative humidity (with respect to ice) retrieved from HIRS channel 12 (6.7 μm) observations for Jul 1989. (bottom) The difference in UTH when a 1-K warm bias is artificially added to the radiative transfer model used to perform the retrieval.

ture corresponds to roughly a 12% relative error in UTH. It is important to note that errors in simulated brightness temperature scale linearly with the *relative* uncertainty in UTH. Hence, a constant error in brightness temperature introduces a smaller *absolute* uncertainty at the dry end of the UTH spectrum and a larger absolute uncertainty at the moist end. This general relationship provides guidance on how the intermodel differences translate into UTH retrieval errors. Figure 6 shows the distribution monthly mean UTH (with respect to ice) derived from HIRS 6.7-μm observations for July 1989 following Soden and Bretherton (1996). The UTH distribution in the top panel was retrieved using the RTTOV-3 model. The bottom panel depicts the difference in the retrieved UTH distribution when a 1-K warm bias was artificially added to the same radiative transfer model. Over the subtropics, where the upper troposphere is relatively dry, the difference in UTH is quite small (< 2% in terms of the absolute difference). On the other hand, over the more humid tropical areas retrievals performed with the biased model clearly overestimate the UTH and exhibit errors that approach 10%. Thus for a given radiance error (ΔT_b), satellite measurements of UTH are actually most reliable (in an absolute sense) under the driest conditions. In contrast, conventional radiosonde measurements of upper-tropospheric water vapor are generally considered to be least reliable at low relative humidities (Elliott and Gaffen 1991).

4. Summary

The relative convergence among the various radiation codes utilized in this workshop represents an advancement in the treatment and understanding of clear-sky radiative processes in this spectral region. The primary conclusions from the workshop may be summarized as follows.

- LBL calculations typically agree to within ~0.2 K with the exception of one model.
- The majority of NB and SB models agree to within ±1 K of reference LBL results. The agreement of the SB models with the reference LBL calculations is improved for newer or more recent versions of SB models.

- Older SB models, particularly those without explicit parameterizations for water vapor continuum absorption, exhibit biases in excess of 2 K. Retrievals of UTH from these models will systematically overestimate the moisture by as much as 20%–30% (relative error).
- For the 6.7-μm channel, SB models (eg., 16 and 20) can provide radiance calculations to the same level of accuracy as LBL models (rms differences of ~0.2 K). This level of accuracy should be the standard that all SB models strive to attain.
- Continuum absorption by H_2O and, to a lesser extent O_2, is important in this spectral region, collectively reducing the simulated brightness temperatures by ~2 K.
- Accurate, simultaneous measurements of both the atmospheric (temperature, water vapor, and trace gas) profiles and spectral radiances are needed to validate the LBL calculations.

In addition to intercomparing radiation codes, the development of accurate UTH climatologies is also an important component of GVaP. At present several different climatologies exist. The characterization of these climatologies in terms of intrinsic errors and uncertainties will require comparison of the satellite retrievals with independent observations. Such efforts are currently under way and will be the subject of future workshops that will include satellite–satellite and satellite–in situ comparisons, as well as studies of satellite calibration and spectral characterization uncertainty.

Acknowledgments. We thank M. Matricardi of ECMWF for providing the diverse profile dataset, and S. A. Clough and two anonymous reviewers for their comments.

References

Berg, W., J. J. Bates, and D. L. Jackson, 1998: Analysis of upper-tropospheric water vapor brightness temperatures from SSM/T2, HIRS, and GMS-5 VISSR. *J. Appl Meteor.,* **38,** 580–595.

Berk, A., L. S. Bernstein, and D. C. Robertson, 1989: MODTRAN: A moderate resolution model for LOWTRAN 7. Tech. Rep. GL-TR-89-0122, 38 pp. [Available from Spectral Sciences, Inc., 99 South Bedford St., Burlington, MA 01803.]

Chaboureau, J. P., A. Chedin, and N. A. Scott, 1998: Remote sensing of the vertical distribution of atmospheric water vapor from the TOVS observations: Method and validation. *J. Geophys. Res.,* **103,** 8743–8752.

Chahine, M. T., 1997: The future direction of the GEWEX global water vapor project. *GEWEX Newsl.,* Vol. 7, No. 4, 1–2.

Chedin, A., N. A. Scott, C. Wahiche, and P. Moulinier, 1985: The improved initialization inversion method: A high resolution physical method for temperature retrievals from satellites of the TIROS-N series. *J. Climate Appl. Meteor.,* **24,** 128–143.

Clough, S. A., and M. J. Iacono, 1995: Line-by-line calculation of atmospheric fluxes and cooling rates. 2: Applications to carbon dioxide, ozone, methane, nitrous oxide and the halocarbons. *J. Geophys. Res.,* **100,** 16 519–16 535.

——, F. X. Kneizys, and R. W. Davies, 1989: Line shape and the water vapor continuum. *Atmos. Res.,* **23,** 229–241.

——, M. J. Iacono, and J.-L. Moncet, 1992: Line-by-line calculation of atmospheric fluxes and cooling rates: Applications to water vapor. *J. Geophys. Res.,* **97,** 15 671–15 785.

Derber, J. C., and W. S. Wu, 1998: The use of TOVS cloud-cleared radiances in the NCEP SSI analysis system. *Mon. Wea. Rev.,* **126,** 2287–2302.

Edwards, D. P., 1992: GENLN2: A general line-by-line atmospherictransmittance and radiance model. NCAR Tech. Note NCAR/TN-367+STR.

Elliott, W. P., and D. J. Gaffen, 1991: On the utility of radiosonde humidity archives for climate studies. *Bull. Amer. Meteor. Soc.,* **72,** 1507–1520.

Engelen, R. J., and G. L. Stephens, 1998: Comparison between TOVS/HIRS and SSM/T-2 derived upper-tropospheric humidity. *Bull. Amer. Meteor. Soc.,* **79,** 2748–2751.

——, and ——, 1999: Characterization of water vapour retrievals from infrared TOVS radiances and microwave SSM/T-2 radiances. *Quart. J. Roy. Meteor. Soc.,* **125,** 331–351.

Eyre, J. R., 1991: A fast radiative transfer model for satellite sounding systems. ECMWF Tech. Memo. 176, European Centre for Medium-Range Weather Forecasts, Reading, United Kingdom, 28 pp.

——, G. A. Kelly, A. P. McNally, E. Anderson, and A. Persson, 1993: Assimilation of TOVS radiances through one-dimensional variational analysis. *Quart. J. Roy. Meteor. Soc.,* **119,** 1427–1463.

Garand, L., and J. Hallé, 1997: Assimilation of clear- and cloudy-sky upper-tropospheric humidity estimates using *GOES-8* and *GOES-9* data. *J. Atmos. Oceanic Technol.,* **14,** 1036–1054.

——, D. S. Turner, C. Chouinard, and J. Halle, 1999: A physical formulation of atmospheric transmittances for the massive assimilation of satellite infrared radiances. *J. Appl. Meteor.,* **38,** 541–554.

Jacquinet-Husson, N., and Coauthors, 1999: The 1997 spectroscopic GEISA databank. *J. Quant. Spect. Radiat. Transfer,* **61,** 425–438.

Jedlovec, G. J., J. A. Lerner, and R. J. Atkinson, 2000: A satellite-derived upper-tropospheric water vapor transport index for climate studies. *J. Appl. Meteor.,* **39,** 15–41.

Joiner, J., H.-T. Lee, L. L. Strow, P. K. Bhartia, S. Hannon, A. J. Miller, and L. G. Rokke, 1998: Radiative transfer in the 9.6 micron HIRS ozone channel using collocated SBUV-determined ozone abundances. *J. Geophys. Res.,* **103,** 19 213–19 219.

Key, J., 1997: Streamer user's guide. Tech. Rep. 96-01, Department of Geography, Boston University, 85 pp.

Kneizys, F. X., and Coauthors, 1983: Atmospheric transmittance radiance code LOWTRAN-6. AFGL-TR-83-0187.

Matricardi, M., and R. W. Saunders, 1999: A fast radiative transfer model for simulation of IASI radiances. *Appl. Opt.,* **38,** 5679–5691.

McMillin, L. M., L. J. Crone, and T. J. Kleespies, 1995: Atmospheric transmittance of an absorbing gas, 5. Improvements to the OPTRAN approach. *Appl. Opt.,* **34,** 8396–8399.

Neuendorffer, A. C., 1997: Rapid atmospheric transmittance through fast Fourier convolution. *J. Opt. Soc. Amer.,* **67,** 1376–1390.

Rothman, L. S., 1993: The HITRAN molecular database: Enhancements for remote sensing, atmospheric propagation and remote sensing II. *SPIE Proc.,* **1968,** 687–694.

Salathe, E. P., and R. B. Smith, 1996: Comparison of 6.7 μm radiance computed from aircraft soundings and observed from GOES. *J. Geophys. Res.,* **101,** 21 303–21 310.

——, and D. L. Hartmann, 1997: A trajectory analysis of tropical upper tropospheric moisture and convection, *J. Climate,* **10,** 2533–2547.

Saunders, R. W., M. Matricardi, and P. Brunel, 1999: An improved fast radiative transfer model for assimilation of satellite radiance observations. *Quart. J. Roy. Meteor. Soc.,* **125,** 1407–1425.

Schmetz, J., and O. M. Turpeinen, 1989: Estimation of the upper tropospheric relative humidity field from METEOSAT water vapor image data. *J. Appl. Meteor.,* **27,** 889–899.

Schwarzkopf, M. D., and V. Ramaswamy, 1999: Radiative effects of CH_4, N_2O, halocarbons, and foreign-broadened H_2O continuum: A GCM experiment. *J. Geophys. Res.,* **104,** 9467–9488.

Scott, N. A., and A. Chedin, 1981: Fast line-by-line method for atmospheric absorption computations: The automated atmospheric absorption atlas. *J. Appl. Meteor.,* **20,** 802–812.

Soden, B. J., and F. P. Bretherton, 1993: Upper tropospheric humidity from the GOES 6.7 μm channel: method and climatology for July 1987. *J. Geophys. Res.,* **98,** 16 669–16 688.

——, and ——, 1996: Interpretation of TOVS water vapor radiances in terms of layer-average relative humidities: Method and climatology for the upper, middle, and lower troposphere. *J. Geophys. Res.,* **101,** 9333–9343.

Spencer, R. W., and W. D. Braswell, 1997: How dry is the tropical free troposphere? Implications for global warming theory. *Bull. Amer. Meteor. Soc.,* **78,** 1097–1106.

Stephens, G. L., D. L. Jackson, and I. Wittmeyer, 1996: Global observations of upper-tropospheric water vapor derived from TOVS radiance data. *J. Climate,* **9,** 305–326.

Strow, L. L., H. E. Motteler, R. G. Benson, S. E. Hannon, and S. De Souza-Machado, 1998: Fast computation of monochromatic infrared atmospheric transmittances using compressed lookup tables. *J. Quant. Spectrosc. Radiat. Transfer,* **59,** 481–493.

Thibault, F., V. Menoux, R. Le Doucen, L. Rosenmann, J.-M. Hartmann, and Ch. Boulet, 1997: Infrared-collision-induced absorption of O_2 near 6.4 μm for atmospheric applications: Measurements and empirical modelling. *Appl. Opt.,* **36,** 563–567.

Timofeyev, Y. M., and M. V. Tonkov, 1978: Effect of the induced oxygen absorption band on the transformation of radiation in the 6 micron region of the earth's atmosphere. *Atmos. Oceanic Phys.,* **14,** 437–441.

Tjemkes, S., and J. Schmetz, 1997: Synthetic satellite radiances using the radiance sampling method. *J. Geophys. Res.,* **102,** 1807–1818.

Tournier, B., R. Armante, and N. A. Scott, 1995: Stransac-93 and 4A-93. Development et validation des nouvelles versions des codes de transfert radiatif pour application au projet IASI. LMD Internal Note 201, 43 pp.

Turner, D. S., 1995: Absorption coefficient estimation using a two-dimensional interpolation procedure. *J. Quant. Spectrosc. Radiat. Transfer,* **53,** 633–637.

Warner, J. X., 1997: A new longwave radiation model for application to atmospheric problems. Ph.D. dissertation, University of Maryland at College Park, College Park, MD, 200 pp.

Weinreb, M. P., H. E. Fleming, L. M. McMillin, and A. C. Neuendorffer, 1981: Transmittances for the TIROS Operational Vertical Sounder. NOAA Tech. Rep. NESS 85, 60 pp.